Nonlinear Dyn (2019) 95:2353–2365
https://doi.org/10.1007/s11071-018-4696-x

ORIGINAL PAPER

Event-triggered feedback control for discrete-time piecewise affine systems subject to input saturation

Yifei Ma · Wei Wu · Daniel Görges · Baotong Cui

Received: 4 April 2018 / Accepted: 1 December 2018 / Published online: 10 December 2018

Abstract The problem of event-triggered control is investigated for discrete-time piecewise affine systems subject to input saturation. Linear matrix inequality (LMI) based on local stability criterion is formed by introducing a nonlinear dead-zone function which represent saturation characteristics. Unique state feedback control gains can be obtained by solving the LMI problem under the event-triggering strategy. The domain of attraction is estimated and maximized with the controller synthesis via ellipsoidal approximations. The effectiveness of controller is illustrated by simulations of numerical examples.

Keywords Event-triggered control · Piecewise affine system · Lyapunov stability · Linear matrix inequality · Input saturation

1 Introduction

Event-triggered control (ETC) has received much attention in recent years due to the advantages of less resource utilization compared to traditional control systems [1–5]. In event-triggered mechanism, the control task is executed through event-induced fashion, where the event is generated by a specific event-triggering condition instead of traditional periodic control. In [6], Årzen first proposed PID control based on an event-triggering strategy, which could greatly reduce the resource utilization. The event-triggering strategy has been studied in detail via simulations and experiments. In [2], the closed-loop system is input-to-output stable in the presence of state error by designing event-triggered state feedback controller. In the literature [7], the periodic event-triggered control (PETC) is investigated where the states need to be monitored according to a fixed period. The data are processed by the event generator at the time of each period to determine whether the controller is updated. Analogically, the same objective is also covered in the self-triggered control strategy [8]. That the self-triggered control computes the next sampling time or update time ahead of time based on the acquired data mainly distinguishes from the event-triggered control [9]. In recent years, ETC has also been applied to hybrid systems [10] and distributed process control of unmanned aerial vehicle [11]. However, few results were addressed for ETC of piecewise affine systems with input saturation. In the following, previous work on the ETC of systems with input saturation and piecewise affine systems will be briefly discussed.

One of the important issues for ETC lies in controller design together with the event-triggering condition. Event-triggered synthesis approaches are researched for discrete-time linear systems with bounded exoge-

Y. Ma · W. Wu (✉) · B. Cui
Key Laboratory of Advanced Process Control for Light Industry (Ministry of Education), Jiangnan University, Wuxi 214122, China
e-mail: weiwu@jiangnan.edu.cn

D. Görges
Department of Electrical and Computer Engineering, University of Kaiserslautern, 67663 Kaiserslautern, Germany

nous disturbance in [12]. In [13], a controller synthesis approach is proposed by regarding a quadratic cost function as the control performance. Recently, event-triggered control has been addressed with input saturation through the different approaches. A procedure is proposed in [5] to design a feedback controller that maximizes the domain of attraction is achieved of the linear system under a given event-triggering condition. In [14], a method of designing a triggering function is proposed to ensure the asymptotic stability of a PI-controlled plant. A cone complementarity linearization algorithm is proposed in [15] for solving the non-convex optimization problem in order to research the co-design of controller with saturation.

Piecewise affine (PWA) systems have wide applications in control systems because they can be considered as a powerful tool for approximating nonlinear systems [16–18]. There have been many existing results on stability analysis and controller design of PWA systems. A method for designing a chaotic generator by using PWA system is proposed in [19]. In [20], the domain information of the current state is included into the stability criteria for reducing conservativeness. A new approach for characterizing domains of attraction for PWA systems based on the discrete transition functions is given in [21]. In [22], an improved Lyapunov–Krasovskii functional method is used to study PWA systems with time delay. A piecewise quadratic Lyapunov function method which is suitable for Lur'e systems is proposed in [23], but the result cannot be directly extended to PWA systems with a more general state space polyhedral partition. In [24], a piecewise Lyapunov function method is proposed by combining the quadratic functions of all the regions dividing the state space. The stability conditions are expressed by the cone-constraint inequality, which can be transformed into an LMI. The problem of robust and reliable H_∞ static output feedback control with time delay is discussed for uncertain PWA systems in [25].

On the other hand, most of the practical controllers are constrained. The controller which ignores the constrained design may reduce the performance of the system and even lead to instability of the system. Therefore, it is necessary to study the control input saturation. In the context of input saturation, an LMI-based robust stability analysis and controller design were presented for discrete-time PWA systems subject to input saturation in [26], where also the domain of attraction is estimated. The literature [27] considers both input and state constraints, and l_2-gain control is studied. And the measurement and maximization of disturbance tolerance is investigated. However, the problem of network data transmission is not considered in the literature. Delay or packet loss of network data transmission will affect the performance of the system. We hope to reduce the waste of network resources as far as possible. Therefore, event-triggered control of piecewise affine system subject to input saturation is proposed in this paper.

This paper considers the controller design under an event-triggering strategy for discrete-time PWA systems with input saturation. The local stability condition is proposed. Then, the event-triggered controller is designed and the problem of estimate the system's domain of attraction is solved. Meanwhile, an optimization approach is given to maximize the domain of attraction. The simulation results show that the size of the domain of attraction is related to a design parameter of the event-triggering condition. Compared with the previous literature in [14,26], the main contributions of this paper are: (i) the stability of the PWA systems with input saturation is addressed by using a sector condition, (ii) the approaches of estimating and maximizing the domain of attraction for PWA systems are proposed, and (iii) the number of controller updates and the waste of network resources are reduced by using event-triggering scheme.

This paper consists of five sections. In Sect. 2, the PWA system is introduced and some preliminary definitions and lemmas are given. The main approach of controller design with input saturation under the event-triggered strategy is proposed in Sect. 3 . Simulations of numerical examples are presented in Sect. 4. Finally, a conclusion is given in Sect. 5.

Notation: $\|\cdot\|$ stands for the Euclidean norm. $\mathrm{tr}(\boldsymbol{X})$ denotes the trace of square matrix $\boldsymbol{X}$ and $\mathrm{diag}(\boldsymbol{X},\boldsymbol{Y})$ denotes a block diagonal matrix. For a symmetric matrix $\boldsymbol{X} \in \mathbb{R}^{n\times n}$, we write $\boldsymbol{X} > 0$ to represent that the matrix $\boldsymbol{X}$ is positive definite. A matrix $\begin{pmatrix} \boldsymbol{A} & * \\ \boldsymbol{B} & \boldsymbol{C} \end{pmatrix}$ represents a symmetric matrix $\begin{pmatrix} \boldsymbol{A} & \boldsymbol{B}^T \\ \boldsymbol{B} & \boldsymbol{C} \end{pmatrix}$.

2 Problem formulation

Considering a discrete-time PWA system with input saturation of the form

$$\begin{cases} \boldsymbol{x}(k+1) = \boldsymbol{A}_i\boldsymbol{x}(k) + \boldsymbol{B}_i\boldsymbol{u}(k) + \boldsymbol{a}_i \\ \boldsymbol{u}(k) = \mathrm{sat}(\boldsymbol{v}(k)) \quad \text{for } \boldsymbol{x}(k) \in \boldsymbol{\chi}_i, i \in \wp, \end{cases} \tag{1}$$

with $\boldsymbol{A}_i \in \mathbb{R}^{n\times n}$ being the system matrix of i-th subsystem, $\boldsymbol{B}_i \in \mathbb{R}^{n\times m}$ being the input matrix of i-th subsystem, $\boldsymbol{a}_i \in \mathbb{R}^n$ being the affine term of i-th subsystem, $\boldsymbol{x}(k) \in \mathbb{R}^n$ being the state vector, $\boldsymbol{u}(k) \in \mathbb{R}^m$ being the control input, and $\boldsymbol{v}(k) \in \mathbb{R}^m$ being a control input signal without saturation. The sat$(\cdot)$ represents the nonlinear saturation function defined by

$$\text{sat}(\boldsymbol{v}(k)) = \begin{cases} -\boldsymbol{u}_0 & \text{if } \boldsymbol{v}(k) < -\boldsymbol{u}_0 \\ \boldsymbol{v}(k) & \text{if } -\boldsymbol{u}_0 \le \boldsymbol{v}(k) \le \boldsymbol{u}_0 \\ \boldsymbol{u}_0 & \text{if } \boldsymbol{u}_0 < \boldsymbol{v}(k), \end{cases} \tag{2}$$

where $\boldsymbol{u}_0$ is the saturated value of the controller under symmetric saturation.

A partition of the state space can be done with closed polyhedral cells $\boldsymbol{\chi}_i = \{\boldsymbol{x} \mid \boldsymbol{L}_i\boldsymbol{x} + \boldsymbol{l}_i \ge 0\}_{i\in\wp} \in \mathbb{R}^n$, with $\boldsymbol{L}_i \in \mathbb{R}^{n\times n}, \boldsymbol{l}_i \in \mathbb{R}^n$. $\wp$ is the index set of these polyhedral cells. $\wp$ can be divided into $\wp = \wp_0 \bigcup \wp_1$, where $\wp_0$ is the set of indices that contains the origin and $\wp_1$ is the set of indices that does not contain origin.

Considering that the evolvement of the trajectory for discrete-time systems may transit from one region to another, let Ω denote index pairs which represent the possible transitions of the state trajectories, that is,

$$\Omega = \{(i,l) \mid \boldsymbol{x}(k) \in \boldsymbol{\chi}_i, \boldsymbol{x}(k+1) \in \boldsymbol{\chi}_l, i, l \in \wp\}.$$

When the state trajectories transmit from region $\boldsymbol{\chi}_i$ to $\boldsymbol{\chi}_l$ at instant k, the system dynamics is determined by the local model dynamics of $\boldsymbol{\chi}_i$.

Remark 1 The main purpose of event-triggered control is to reduce data transmission. In ETC, the task is executed when the event occurs, by violating the specific event-triggering condition. When the event-triggering condition (6) is violated, the event is triggered. The memory saves the state value of the current step. Otherwise, the controller is obtained by using the state value of the last event triggered by the memory. The ZOH in Fig. 1 can be seen as the memory. As shown in Fig. 1, when the event occurs, the switch is closed. The state is transmitted through ZOH to the controller and ZOH updates the state value. When the event does not occur, the switch is open and the ZOH keeps the state value of the last event. So, the controller is not updated.

An ellipsoidal description of PWA systems is often used to approximate the polyhedral cells. The ellipsoidal description requires less parameters than polytopic description, and it can establish LMI-based conditions to solve controller synthesis problems in an easy way. To describe the ellipsoid, we assume that there exist matrices $\boldsymbol{E}_i \in \mathbb{R}^{m\times n}$ and $\boldsymbol{f}_i \in \mathbb{R}^m$ such that $\boldsymbol{\chi}_i \subseteq \boldsymbol{\varepsilon}_i$, where

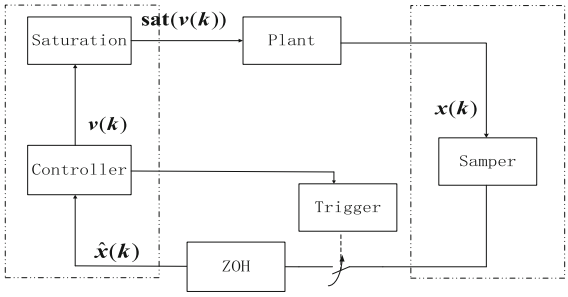

Fig. 1 Closed-loop event-triggered control

$$\boldsymbol{\varepsilon}_i = \{\boldsymbol{x} \mid\mid \boldsymbol{E}_i\boldsymbol{x} + \boldsymbol{f}_i \mid\mid \le 1, i \in \wp\}. \tag{3}$$

The ellipsoids $\boldsymbol{\varepsilon}_i$ can be rewritten as

$$\begin{pmatrix} \boldsymbol{x} \\ 1 \end{pmatrix}^T \begin{pmatrix} \boldsymbol{E}_i^T\boldsymbol{E}_i & * \\ \boldsymbol{f}_i^T\boldsymbol{E}_i & \boldsymbol{f}_i^T\boldsymbol{f}_i - 1 \end{pmatrix} \begin{pmatrix} \boldsymbol{x} \\ 1 \end{pmatrix} \le 0. \tag{4}$$

Specially, when each polyhedral cell $\boldsymbol{\chi}_i$ is a slab, called *piecewise affine slab system*. If $\boldsymbol{\chi}_i = \{\boldsymbol{x} \mid d_1 < c_i^T\boldsymbol{x} < d_2\}$, then the ellipsoidal matrices $\boldsymbol{E}_i, \boldsymbol{f}_i$ can be given by $\boldsymbol{E}_i = 2c_i^T/(d_2 - d_1)$ and $\boldsymbol{f}_i = -(d_2 + d_1)/(d_2 - d_1)$ via the degenerate ellipsoid [28,29].

In this paper, the state feedback control law is considered as

$$\hat{\boldsymbol{v}}(k) = \boldsymbol{K}_i\hat{\boldsymbol{x}}(k) + \boldsymbol{m}_i, \tag{5}$$

where $\boldsymbol{K}_i \in \mathbb{R}^{m\times n}$ and $\boldsymbol{m}_i \in \mathbb{R}^m$ are controller gains of i-th subsystem designed later, and $\hat{\boldsymbol{x}}(k)$ indicates the state value of the last event-triggered defined by

$$\hat{\boldsymbol{x}}(k) = \begin{cases} \boldsymbol{x}(k) & \text{if } \boldsymbol{v}(k) \text{ is updated} \\ \hat{\boldsymbol{x}}(k-1) & \text{if } \boldsymbol{v}(k) \text{ is not updated.} \end{cases} \tag{6}$$

The event-triggering condition for the PWA system (1) will be given in Sect. 3.

We define the event-triggering time as:

$$k_0, k_1, k_2, \ldots, k_d, k_{d+1}, \ldots$$

so the (6) can be rewritten as

$$\hat{\boldsymbol{x}}(k) = \begin{cases} \boldsymbol{x}(k_{d+1}) & \text{if } k = k_{d+1} \\ \boldsymbol{x}(k_d) & \text{if } k \in [k_d\ k_{d+1}). \end{cases} \tag{7}$$

$k = k_d$ and $k = k_{d+1}$ represent that the system is at the time of event triggering. $k \in (k_d\ k_{d+1})$ indicates that the system is between two event-triggered time.

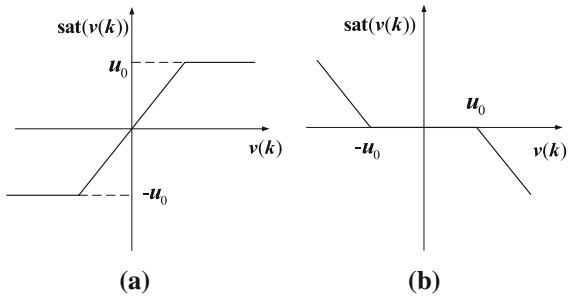

Fig. 2 **a** Saturation nonlinearity and **b** dead-zone nonlinearity

The error variable is defined as

$$\begin{aligned} \boldsymbol{e}(k) &= \hat{\boldsymbol{v}}(k) - \boldsymbol{v}(k) \\ &= \boldsymbol{K}_j \hat{\boldsymbol{x}}(k) + \boldsymbol{m}_j - \boldsymbol{K}_i \boldsymbol{x}(k) - \boldsymbol{m}_i, i, j \in \wp \end{aligned} \tag{8}$$

where $\boldsymbol{e}(k)$ is the input difference between the value of controller update when the last event is triggered and the actual desired control effect. We assume that the state of system is located in the j-th subsystem when last event occurs and in the i-th subsystem of current step ($j = i$ or $j \neq i$). $\boldsymbol{K}_j, \boldsymbol{m}_j$ are controller gains designed for the j-th subsystem when the last event triggers. $\boldsymbol{K}_i, \boldsymbol{m}_i$ are controller gains designed for the i-th subsystem. $\hat{\boldsymbol{x}}(k)$ indicates the state value saved by ZOH when the last event occurred. $\hat{\boldsymbol{v}}(k)$ is the updated value of the controller when the last event occurred. $\boldsymbol{v}(k)$ is actual desired control effect.

In order to transform the saturation nonlinearity into dead-zone nonlinearity, a dead-zone function is defined by

$$\text{sat}(\boldsymbol{v}(k)) = \phi(\boldsymbol{v}(k)) + \boldsymbol{v}(k), \tag{9}$$

with

$$\phi(\boldsymbol{v}(k)) = \begin{cases} -\boldsymbol{u}_0 - \boldsymbol{v}(k) & \text{for } \boldsymbol{v}(k) < -\boldsymbol{u}_0 \\ \boldsymbol{0} & \text{for } -\boldsymbol{u}_0 \leq \boldsymbol{v}(k) \leq \boldsymbol{u}_0 \\ \boldsymbol{u}_0 - \boldsymbol{v}(k) & \text{for } \boldsymbol{u}_0 < \boldsymbol{v}(k). \end{cases}$$

The saturation nonlinearity characteristics for $\text{sat}(\boldsymbol{v}(k))$ and for $\phi(\boldsymbol{v}(k))$ are shown in Fig. 2.

The system (1) with the substitution of (8) and (9) is equivalent to

$$\boldsymbol{x}(k+1) = \overline{\boldsymbol{A}}_i \boldsymbol{x}(k) + \boldsymbol{B}_i \boldsymbol{e}(k) + \boldsymbol{B}_i \phi(\boldsymbol{v}(k)) + \overline{\boldsymbol{a}}_i, \tag{10}$$

where $\overline{\boldsymbol{A}}_i = \boldsymbol{A}_i + \boldsymbol{B}_i \boldsymbol{K}_i, \overline{\boldsymbol{a}}_i = \boldsymbol{B}_i \boldsymbol{m}_i + \boldsymbol{a}_i$.

The following are definitions and lemmas used in the paper.

Definition 1 Given a symmetric matrix $\boldsymbol{P}_i > 0, i \in \wp$ and a scalar $\rho > 0$, the set $\xi(\boldsymbol{P}_i, \rho)$ represents the ellipsoid

$$\xi(\boldsymbol{P}_i, \rho) = \{\boldsymbol{x} \in \mathbb{R}^n : \boldsymbol{x}^T \boldsymbol{P}_i \boldsymbol{x} \leq \rho\}. \tag{11}$$

Definition 2 A region $\boldsymbol{\chi}_i$ is a region of asymptotic stability (RAS) with respect to the origin of system (1) if $0 \in \boldsymbol{\chi}_i$ and $\boldsymbol{x}(k) \to 0$ as $k \to \infty \, \forall \boldsymbol{x}_0 \in \boldsymbol{\chi}_i$.

Due to the existence of controller saturation nonlinearity, regional asymptotic stability of PWA system can be achieved instead of the global asymptotic stability. Therefore, the domain of attraction defined as $\bigcup_{i \in \wp} (\xi(\boldsymbol{P}_i, 1) \bigcap \boldsymbol{\chi}_i)$ is estimated by the ellipsoidal approximation.

Lemma 1 [30] *For all $\boldsymbol{v}, \boldsymbol{\omega} \in \mathbb{R}^m$, if $\boldsymbol{v}$ and $\boldsymbol{\omega}$ are elements of the set which is defined as*

$$S(\boldsymbol{v} - \boldsymbol{\omega}, -\boldsymbol{u}_0, \boldsymbol{u}_0) = \{-\boldsymbol{u}_0 \leq (\boldsymbol{v} - \boldsymbol{\omega}) \leq \boldsymbol{u}_0\},$$

for the dead-zone nonlinearity $\phi(\boldsymbol{v}(k))$, the following inequality holds

$$\phi^T(\boldsymbol{v}(k)) \boldsymbol{T} (\phi(\boldsymbol{v}(k)) + \boldsymbol{\omega}) \leq 0, \tag{12}$$

where $\boldsymbol{T} \in \mathbb{R}^{m \times m}$ is a diagonal positive definite matrix and $\boldsymbol{\omega} = \boldsymbol{H}_i \boldsymbol{x} + \boldsymbol{g}_i$, with $\boldsymbol{H}_i \in \mathbb{R}^{m \times n}, \boldsymbol{g}_i \in \mathbb{R}^m$.

Remark 2 For asymmetric saturation, i.e., $\boldsymbol{u}_{\min} \neq \boldsymbol{u}_{\max}$. The saturation function (2) becomes

$$\text{sat}(\boldsymbol{v}(k)) = \begin{cases} -\boldsymbol{u}_{\min} & \text{if } \boldsymbol{v}(k) < -\boldsymbol{u}_{\min} \\ \boldsymbol{v}(k) & \text{if } -\boldsymbol{u}_{\min} \leq \boldsymbol{v}(k) \leq \boldsymbol{u}_{\max} \\ \boldsymbol{u}_{\max} & \text{if } \boldsymbol{u}_{\max} < \boldsymbol{v}(k), \end{cases} \tag{13}$$

where $-\boldsymbol{u}_{\min}, \boldsymbol{u}_{\max} \in \mathbb{R}^m$ are the minimum and maximum values of the saturated control input, respectively. Asymmetric saturation of the controller can be converted to symmetric saturation by translating the coordinate system, i.e.,

$$\boldsymbol{u}_{\min} + \overline{\boldsymbol{u}} = \boldsymbol{u}_{\max} - \overline{\boldsymbol{u}} = \boldsymbol{u}_0, \tag{14}$$

where $\overline{\boldsymbol{u}}$ is a vector of $\mathbb{R}^m$. Without loss of generality, we mainly discuss the symmetric saturation of the controller.

Considering the system (1) with the input saturation of the formulation (2), the input saturation problem is effectively solved by designing an event-triggered controller while reducing the number of event triggers

which is the number of controller updates. Figure 1 describes the network data transmission of a closed-loop system, and by using ETC the number of data transmission between nodes is reduced, thereby saving communication bandwidth and resources. Thus, the problem can be formalized as

Problem 1 *Design the controller gains for a given σ in the event-triggering strategy (6) to ensure that the system (1) is locally asymptotically stable with input saturation for any initial condition, while the number of control input updates is reduced.*

3 Main result

An event-triggering strategy is proposed, and the event-triggered controller of form (5) is designed based on the strategy such that system (1) is regional stable in a target set via a quadratic Lyapunov function.

Whether the control signal $\boldsymbol{v}(k)$ is updated depends on the event generator which is given by

$$\|\boldsymbol{e}(k)\| \leq \sigma \|\boldsymbol{K}_i \boldsymbol{x}(k) + \boldsymbol{m}_i\|, \tag{15}$$

where $\sigma \in (0, 1)$. Based on the event generator (15), the event-triggering condition can be written as

$$\hat{\boldsymbol{x}}(k) = \begin{cases} \boldsymbol{x}(k) & \text{if} \quad \|\boldsymbol{e}(k)\| > \sigma \|\boldsymbol{K}_i \boldsymbol{x}(k) + \boldsymbol{m}_i\| \\ \hat{\boldsymbol{x}}(k-1) & \text{if} \quad \|\boldsymbol{e}(k)\| \leq \sigma \|\boldsymbol{K}_i \boldsymbol{x}(k) + \boldsymbol{m}_i\|. \end{cases} \tag{16}$$

Remark 3 For a set-point control, the reference state $\boldsymbol{x}_{eq}$ can be shifted to the origin. The event generator is adapted as

$$\|\boldsymbol{e}(k)\| \leq \sigma \|\boldsymbol{K}_i (\boldsymbol{x}(k) - \boldsymbol{x}_{eq}) + \boldsymbol{m}_i\|. \tag{17}$$

Next, we give a theorem which provides a solution to Problem 1.

Theorem 1 *For a given σ in event-triggering strategy (15), if there exist a diagonal positive definite matrix $\boldsymbol{T} \in \mathbb{R}^{m\times m}$, symmetric and positive definite matrix $\boldsymbol{Q}_i \in \mathbb{R}^{n\times n}$, matrices $\boldsymbol{W}_i, \boldsymbol{G}_i \in \mathbb{R}^{m\times n}$, $\boldsymbol{\varpi}_i, \boldsymbol{h}_i \in \mathbb{R}^m$ and scalars $\alpha_i > 0$, $\beta_i > 0$, $i, l \in \wp$ such that the following LMIs hold*

$$\begin{pmatrix} \boldsymbol{Q}_i + \boldsymbol{Q}_i \overline{\boldsymbol{E}}_i^{1/2} + \overline{\boldsymbol{E}}_i^{1/2} \boldsymbol{Q}_i - \beta_i \boldsymbol{I} & * & * & * & * & * \\ \boldsymbol{0} & \alpha_i \boldsymbol{I} & * & * & * & * \\ 2\boldsymbol{T}\boldsymbol{G}_i & \boldsymbol{0} & 2\boldsymbol{T} & * & * & * \\ \boldsymbol{f}_i^T \boldsymbol{E}_i \boldsymbol{Q}_i & \boldsymbol{0} & 2\boldsymbol{T}\boldsymbol{h}_i & \beta_i \boldsymbol{f}_i^T \boldsymbol{f}_i - \beta_i & * & * \\ \boldsymbol{A}_i \boldsymbol{Q}_i + \boldsymbol{B}_i \boldsymbol{W}_i & \alpha_i \boldsymbol{B}_i & \boldsymbol{B}_i & \beta_i \overline{\boldsymbol{a}}_i & \boldsymbol{P}_l^{-1} & * \\ \boldsymbol{W}_i & \boldsymbol{0} & \boldsymbol{0} & \boldsymbol{\varpi}_i & \boldsymbol{0} & \frac{\alpha_i}{\sigma^2} \boldsymbol{I} \end{pmatrix} > 0, \; for \; l \in \wp_1, (i, l) \in \Omega, \tag{18a}$$

$$\begin{pmatrix} \boldsymbol{Q}_i & * & * & * & * \\ \boldsymbol{0} & \alpha_i \boldsymbol{I} & * & * & * \\ 2\boldsymbol{T}\boldsymbol{G}_i & \boldsymbol{0} & 2\boldsymbol{T} & * & * \\ \boldsymbol{A}_i \boldsymbol{Q}_i + \boldsymbol{B}_i \boldsymbol{W}_i & \alpha_i \boldsymbol{B}_i & \boldsymbol{B}_i & \boldsymbol{Q}_l & * \\ \boldsymbol{W}_i & \boldsymbol{0} & \boldsymbol{0} & \boldsymbol{0} & \frac{\alpha_i}{\sigma^2} \boldsymbol{I} \end{pmatrix} > 0, \; for \; l \in \wp_0, (i, l) \in \Omega, \tag{18b}$$

$$\begin{pmatrix} \boldsymbol{Q}_i & * & * \\ \boldsymbol{0} & \boldsymbol{0} & * \\ \boldsymbol{W}_{i(j)} - \boldsymbol{G}_{i(j)} & \boldsymbol{\varpi}_{i(j)} - \boldsymbol{h}_{i(j)} & \boldsymbol{u}_{0(j)}^2 \end{pmatrix} \geq 0, \tag{19}$$

$for \; i \in \wp, j \in [1, m],$

where $\boldsymbol{W}_{i(j)}$, $\boldsymbol{G}_{i(j)}$, $\boldsymbol{\varpi}_{i(j)}$, $\boldsymbol{h}_{i(j)}$ are the j-th row of $\boldsymbol{W}_i$, $\boldsymbol{G}_i$, $\boldsymbol{\varpi}_i$, $\boldsymbol{h}_i$. Then, the PWA system (1) is locally asymptotically stable with $\boldsymbol{K}_i = \boldsymbol{W}_i \boldsymbol{P}_i$, $\boldsymbol{P}_i = \boldsymbol{Q}_i^{-1}$ and region $\bigcup_{i\in\wp}(\xi(\boldsymbol{P}_i, 1) \bigcap \boldsymbol{\chi}_i)$ is a RAS for system (1) under the event-triggering strategy (15).

Proof Assuming that the state $\boldsymbol{x}(k)$ transits from region $\boldsymbol{\chi}_i$ to $\boldsymbol{\chi}_l$, $i, l \in \wp$, and considering a piecewise quadratic Lyapunov function $V = \boldsymbol{x}^T \boldsymbol{P}_i \boldsymbol{x}$, and $\Delta V = \boldsymbol{x}^T(k+1) \boldsymbol{P}_l \boldsymbol{x}(k+1) - \boldsymbol{x}^T(k) \boldsymbol{P}_i \boldsymbol{x}(k)$. Assuming that $\boldsymbol{x} \in S(\boldsymbol{v} - \boldsymbol{\omega}, -\boldsymbol{u}_0, \boldsymbol{u}_0)$ and applying Lemma 1, we can write

$$\Delta V \leq \Delta V - 2\phi^T(\boldsymbol{v}(k)) \boldsymbol{T}(\phi(\boldsymbol{v}(k)) + \boldsymbol{\omega}). \tag{20}$$

Thus, after some algebraic manipulations, we get

$$\Delta V \leq \begin{pmatrix} \boldsymbol{x}(k) \\ \boldsymbol{e}(k) \\ \phi(\boldsymbol{v}(k)) \\ 1 \end{pmatrix}^T \boldsymbol{M} \begin{pmatrix} \boldsymbol{x}(k) \\ \boldsymbol{e}(k) \\ \phi(\boldsymbol{v}(k)) \\ 1 \end{pmatrix}, \tag{21}$$

with

$$\boldsymbol{M}=\begin{pmatrix}\overline{\boldsymbol{A}}_i^T\boldsymbol{P}_l\overline{\boldsymbol{A}}_i-\boldsymbol{P}_i & * & * & *\\ \boldsymbol{B}_i^T\boldsymbol{P}_l\overline{\boldsymbol{A}}_i & \boldsymbol{B}_i^T\boldsymbol{P}_l\boldsymbol{B}_i & * & *\\ \boldsymbol{B}_i^T\boldsymbol{P}_l\overline{\boldsymbol{A}}_i-2\boldsymbol{T}\boldsymbol{H}_i & \boldsymbol{B}_i^T\boldsymbol{P}_l\boldsymbol{B}_i & \boldsymbol{B}_i^T\boldsymbol{P}_l\boldsymbol{B}_i-2\boldsymbol{T} & *\\ \overline{\boldsymbol{a}}_i^T\boldsymbol{P}_l\overline{\boldsymbol{A}}_i & \overline{\boldsymbol{a}}_i^T\boldsymbol{P}_l\boldsymbol{B}_i & \overline{\boldsymbol{a}}_i^T\boldsymbol{P}_l\boldsymbol{B}_i-2\boldsymbol{T}\boldsymbol{g}_i & \overline{\boldsymbol{a}}_i^T\boldsymbol{P}_l\overline{\boldsymbol{a}}_i\end{pmatrix}. \tag{22}$$

Therefore, $\Delta V\le 0$ can be obtained as long as $\boldsymbol{M}\le 0$.

The event-triggering condition is

$$\boldsymbol{e}^T(k)\boldsymbol{e}(k)\le\sigma^2(\boldsymbol{K}_i\boldsymbol{x}(k)+\boldsymbol{m}_i)^T(\boldsymbol{K}_i\boldsymbol{x}(k)+\boldsymbol{m}_i), \tag{23}$$

which is equivalent to

$$\begin{pmatrix}\boldsymbol{x}(k)\\ \boldsymbol{e}(k)\\ \phi(\boldsymbol{v})\\ 1\end{pmatrix}^T\begin{pmatrix}\sigma^2\boldsymbol{K}_i^T\boldsymbol{K}_i & * & \boldsymbol{0} & *\\ \boldsymbol{0} & -\boldsymbol{I} & \boldsymbol{0} & *\\ \boldsymbol{0} & \boldsymbol{0} & \boldsymbol{0} & \boldsymbol{0}\\ \sigma^2\boldsymbol{m}_i^T\boldsymbol{K}_i & \boldsymbol{0} & \boldsymbol{0} & \sigma^2\boldsymbol{m}_i^T\boldsymbol{m}_i\end{pmatrix}\begin{pmatrix}\boldsymbol{x}(k)\\ \boldsymbol{e}(k)\\ \phi(\boldsymbol{v})\\ 1\end{pmatrix}\ge 0. \tag{24}$$

With the S-procedure, we combine (4), (22) and (24) to

$$\begin{pmatrix}\boldsymbol{P}_i-\overline{\boldsymbol{A}}_i^T\boldsymbol{P}_l\overline{\boldsymbol{A}}_i-\kappa_i\sigma^2\boldsymbol{K}_i^T\boldsymbol{K}_i+\gamma_i\boldsymbol{E}_i^T\boldsymbol{E}_i & * & * & *\\ -\boldsymbol{B}_i^T\boldsymbol{P}_l\overline{\boldsymbol{A}}_i & -\boldsymbol{B}_i^T\boldsymbol{P}_l\boldsymbol{B}_i+\kappa_i\boldsymbol{I} & * & *\\ 2\boldsymbol{T}\boldsymbol{H}_i-\boldsymbol{B}_i^T\boldsymbol{P}_l\overline{\boldsymbol{A}}_i & -\boldsymbol{B}_i^T\boldsymbol{P}_l\boldsymbol{B}_i & 2\boldsymbol{T}-\boldsymbol{B}_i^T\boldsymbol{P}_l\boldsymbol{B}_i & *\\ -\overline{\boldsymbol{a}}_i^T\boldsymbol{P}_l\overline{\boldsymbol{A}}_i-\kappa_i\sigma^2\boldsymbol{m}_i^T\boldsymbol{K}_i+\gamma_i\boldsymbol{f}_i^T\boldsymbol{E}_i & -\overline{\boldsymbol{a}}_i^T\boldsymbol{P}_l\boldsymbol{B}_i & 2\boldsymbol{T}\boldsymbol{g}_i-\overline{\boldsymbol{a}}_i^T\boldsymbol{P}_l\boldsymbol{B}_i & \gamma_i\boldsymbol{f}_i^T\boldsymbol{f}_i-\gamma_i-\overline{\boldsymbol{a}}_i^T\boldsymbol{P}_l\overline{\boldsymbol{a}}_i-\kappa_i\sigma^2\boldsymbol{m}_i^T\boldsymbol{m}_i\end{pmatrix}>0. \tag{25}$$

Applying the Schur complement again leads to

$$\begin{pmatrix}\boldsymbol{P}_i+\gamma_i\boldsymbol{E}_i^T\boldsymbol{E}_i & * & * & * & * & *\\ \boldsymbol{0} & \kappa_i\boldsymbol{I} & * & * & * & *\\ 2\boldsymbol{T}\boldsymbol{H}_i & \boldsymbol{0} & 2\boldsymbol{T} & * & * & *\\ \gamma_i\boldsymbol{f}_i^T\boldsymbol{E}_i & \boldsymbol{0} & 2\boldsymbol{T}\boldsymbol{g}_i & \gamma_i\boldsymbol{f}_i^T\boldsymbol{f}_i-\gamma_i & * & *\\ \overline{\boldsymbol{A}}_i & \boldsymbol{B}_i & \boldsymbol{B}_i & \overline{\boldsymbol{a}}_i & \boldsymbol{P}_l^{-1} & *\\ \boldsymbol{K}_i & \boldsymbol{0} & \boldsymbol{0} & \boldsymbol{m}_i & \boldsymbol{0} & \frac{1}{\kappa_i\sigma^2}\boldsymbol{I}\end{pmatrix}>0. \tag{26}$$

Pre-/post-multiplying by diag $\left(\boldsymbol{P}_i^{-1},\frac{1}{\kappa_i},\boldsymbol{I},\frac{1}{\gamma_i},\boldsymbol{I},\boldsymbol{I}\right)$, which as a congruence transformation, (26) results in

$$\begin{pmatrix}\boldsymbol{P}_i^{-1}+\gamma_i\boldsymbol{P}_i^{-1}\boldsymbol{E}_i^T\boldsymbol{E}_i\boldsymbol{P}_i^{-1} & * & * & * & * & *\\ \boldsymbol{0} & \frac{1}{\kappa_i}\boldsymbol{I} & * & * & * & *\\ 2\boldsymbol{T}\boldsymbol{H}_i\boldsymbol{P}_i^{-1} & \boldsymbol{0} & 2\boldsymbol{T} & * & * & *\\ \boldsymbol{f}_i^T\boldsymbol{E}_i\boldsymbol{P}_i^{-1} & \boldsymbol{0} & 2\boldsymbol{T}\boldsymbol{h}_i & \frac{1}{\gamma_i}\boldsymbol{f}_i^T\boldsymbol{f}_i-\frac{1}{\gamma_i} & * & *\\ \boldsymbol{A}_i\boldsymbol{P}_i^{-1}+\boldsymbol{B}_i\boldsymbol{K}_i\boldsymbol{P}_i^{-1} & \frac{1}{\kappa_i}\boldsymbol{B}_i & \boldsymbol{B}_i & \frac{1}{\gamma_i}\overline{\boldsymbol{a}}_i & \boldsymbol{P}_l^{-1} & *\\ \boldsymbol{K}_i\boldsymbol{P}_i^{-1} & \boldsymbol{0} & \boldsymbol{0} & \frac{1}{\gamma_i}\boldsymbol{m}_i & \boldsymbol{0} & \frac{1}{\kappa_i\sigma^2}\boldsymbol{I}\end{pmatrix}>0. \tag{27}$$

The following inequality holds

$$(\gamma_i^{-1}\boldsymbol{I}-\overline{\boldsymbol{E}}_i^{1/2}\boldsymbol{Q}_i)^T\gamma_i\boldsymbol{I}(\gamma_i^{-1}\boldsymbol{I}-\overline{\boldsymbol{E}}_i^{1/2}\boldsymbol{Q}_i)\ge 0. \tag{28}$$

The inequality (28) is equivalent to

$$\gamma_i\boldsymbol{Q}_i\overline{\boldsymbol{E}}_i\boldsymbol{Q}_i\ge\boldsymbol{Q}_i\overline{\boldsymbol{E}}_i^{1/2}+\overline{\boldsymbol{E}}_i^{1/2}\boldsymbol{Q}_i-\gamma_i^{-1}\boldsymbol{I}. \tag{29}$$

For $l\in\wp_0$, note that $\boldsymbol{m}_i, i\in\wp$ must be chosen as $\boldsymbol{0}$. Through similar derivation, the LMI can be written as (18b).

Therefore, (27) is transformed to (18a) by substituting $\boldsymbol{W}_i=\boldsymbol{K}_i\boldsymbol{P}_i^{-1}$, $\boldsymbol{G}_i=\boldsymbol{H}_i\boldsymbol{P}_i^{-1}$, $\boldsymbol{\varpi}_i=\beta_i\boldsymbol{m}_i$, $\boldsymbol{h}_i=\beta_i\boldsymbol{g}_i$, $\boldsymbol{Q}_i=\boldsymbol{P}_i^{-1}$ and $\overline{\boldsymbol{E}}_i=\boldsymbol{E}_i^T\boldsymbol{E}_i$, $\alpha_i=\frac{1}{\kappa_i}$, $\beta_i=\frac{1}{\gamma_i}$.

Now, we show that (19) ensures $\boldsymbol{x}\in S(\boldsymbol{v}-\boldsymbol{\omega},-\boldsymbol{u}_0,\boldsymbol{u}_0)$, providing $\boldsymbol{x}(0)\in\bigcup_{i\in\wp}(\xi(\boldsymbol{P}_i,1)\bigcap\boldsymbol{\chi}_i)$.

Pre- and post-multiplying (19) by the diag $\begin{pmatrix}\boldsymbol{P}_i & \gamma_i\boldsymbol{I} & \boldsymbol{I}\end{pmatrix}$ and applying Schur complement twice, the following inequality holds for $j=1,\ldots,m$

$$\begin{pmatrix}\boldsymbol{P}_i & \boldsymbol{0}\\ \boldsymbol{0} & \boldsymbol{0}\end{pmatrix}-\left((\boldsymbol{K}_{i(j)}-\boldsymbol{H}_{i(j)})\ (\boldsymbol{m}_{i(j)}-\boldsymbol{g}_{i(j)})\right)^T\frac{1}{\boldsymbol{u}_{0(j)}^2}\left((\boldsymbol{K}_{i(j)}-\boldsymbol{H}_{i(j)})\ (\boldsymbol{m}_{i(j)}-\boldsymbol{g}_{i(j)})\right)\ge 0. \tag{30}$$

Pre- and post-multiplying (30) by $\begin{pmatrix}\boldsymbol{x}\\ 1\end{pmatrix}^T$ and $\begin{pmatrix}\boldsymbol{x}\\ 1\end{pmatrix}$, respectively, (30) implies that

$$\boldsymbol{x}^T\boldsymbol{P}_i\boldsymbol{x}-[(\boldsymbol{K}_{i(j)}-\boldsymbol{H}_{i(j)})\boldsymbol{x}+(\boldsymbol{m}_{i(j)}-\boldsymbol{g}_{i(j)})]^T\frac{1}{\boldsymbol{u}_{0(j)}^2}[(\boldsymbol{K}_{i(j)}-\boldsymbol{H}_{i(j)})\boldsymbol{x}+(\boldsymbol{m}_{i(j)}-\boldsymbol{g}_{i(j)})]\ge 0. \tag{31}$$

By substituting $\boldsymbol{v}=\boldsymbol{K}_i\boldsymbol{x}+\boldsymbol{m}_i$ and $\boldsymbol{\omega}=\boldsymbol{H}_i\boldsymbol{x}+\boldsymbol{g}_i$, (31) is transformed into

$$\|\boldsymbol{v}-\boldsymbol{\omega}\|\le\boldsymbol{u}_0^2\boldsymbol{x}^T\boldsymbol{P}_i\boldsymbol{x}. \tag{32}$$

If $\boldsymbol{x}(k)\in\xi(\boldsymbol{P}_i,1)\le 1$ at instant k, $\boldsymbol{x}(k)\in S(\boldsymbol{v}-\boldsymbol{\omega},-\boldsymbol{u}_0,\boldsymbol{u}_0)$ can be concluded. Hence, we can conclude that if $\boldsymbol{x}(0)\in\xi(\boldsymbol{P}_i,1), i\in\wp$, (19) effectively guarantees that $\boldsymbol{x}(k)\in S(\boldsymbol{v}-\boldsymbol{\omega},-\boldsymbol{u}_0,\boldsymbol{u}_0)$

and $\Delta V \leq 0\ \forall k \geq 0$, which guarantees that $\bigcup_{i\in\wp}(\xi(\boldsymbol{P}_i,1)\bigcap\boldsymbol{\chi}_i)$ is domain of attraction of system (1). That is, all trajectories of system (1) will remain in the set $\bigcup_{i\in\wp}(\xi(\boldsymbol{P}_i,1)\bigcap\boldsymbol{\chi}_i)$.

This completes the proof. □

Remark 4 The controller designed in our paper is expressed as $\hat{\boldsymbol{v}}(k)=\boldsymbol{K}_i\hat{\boldsymbol{x}}(k)+\boldsymbol{m}_i$. The role of $\boldsymbol{m}_i$ is to handle affine item $\boldsymbol{a}_i$ in the i-th subsystem. We define that $\wp_0$ is the set of indices that contains the origin. $i\in\wp_0$ indicates that the i-th subsystem contains the origin. That is, $\boldsymbol{a}_i=0$ and the i-th subsystem is a linear system like $\boldsymbol{x}(k+1)=\boldsymbol{A}_i\boldsymbol{x}(k)+\boldsymbol{B}_i\hat{\boldsymbol{v}}(k)$. Therefore, the controller in the i-th subsystem is defined for a linear system. The controller is defined as $\hat{\boldsymbol{v}}(k)=\boldsymbol{K}_i\hat{\boldsymbol{x}}(k)$.

Remark 5 We use the interior point algorithm to solve LMIs in Theorem 1. The number of free scalar variables is $N=(n+1)(n+2m)+m$, where n represents the dimension of the system and m represents the dimension of the controller.

The regional asymptotic stability of the PWA system (1) is achieved by Theorem 1 regardless of $\boldsymbol{A}_i, i\in\wp$ being Hurwitz. However, if matrix $\boldsymbol{A}_i, i\in\wp$ is Hurwitz, global asymptotic stability can be achieved. This result is not a trivial simplification of Theorem 1 since the PWA system also can be modeled as switched system, where the switched system may be unstable even though each subsystem $\boldsymbol{A}_i$ is Hurwitz [31]. Therefore, a corollary is given as follows.

Corollary 1 *For a given σ in event-triggering strategy (15), if there exist a diagonal positive definite matrix $\boldsymbol{T}\in\mathbb{R}^{m\times m}$, symmetric and positive definite matrix $\boldsymbol{Q}_i\in\mathbb{R}^{n\times n}$, matrices $\boldsymbol{W}_i\in\mathbb{R}^{m\times n}$, $\boldsymbol{\varpi}_i\in\mathbb{R}^m$ and scalars $\alpha_i>0$, $\beta_i>0$, $i,l\in\wp$, such that the following LMIs hold*

$$\begin{pmatrix}
\boldsymbol{Q}_i+\boldsymbol{Q}_i\overline{\boldsymbol{E}}_i^{1/2}+\overline{\boldsymbol{E}}_i^{1/2}\boldsymbol{Q}_i-\beta_i\boldsymbol{I} & * & * & * & * & * \\
\boldsymbol{0} & \alpha_i\boldsymbol{I} & * & * & * & * \\
2\boldsymbol{T}\boldsymbol{W}_i & \boldsymbol{0} & 2\beta_i\boldsymbol{T} & * & * & * \\
\boldsymbol{f}_i^T\boldsymbol{E}_i\boldsymbol{Q}_i & \boldsymbol{0} & 2\boldsymbol{T}\boldsymbol{\varpi}_i & \beta_i\boldsymbol{f}_i^T\boldsymbol{f}_i-\beta_i & * & * \\
\boldsymbol{A}_i\boldsymbol{Q}_i+\boldsymbol{B}_i\boldsymbol{W}_i & \alpha_i\boldsymbol{B}_i & \beta_i\boldsymbol{B}_i & \beta_i\overline{\boldsymbol{a}}_i & \boldsymbol{Q}_l & * \\
\boldsymbol{W}_i & \boldsymbol{0} & \boldsymbol{0} & \boldsymbol{\varpi}_i & \boldsymbol{0} & \frac{\alpha_i}{\sigma^2}\boldsymbol{I}
\end{pmatrix}>0,\ for\ \ l\in\wp_1,(i,l)\in\Omega, \tag{33a}$$

$$\begin{pmatrix}
\boldsymbol{Q}_i & * & * & * & * \\
\boldsymbol{0} & \alpha_i\boldsymbol{I} & * & * & * \\
2\boldsymbol{T}\boldsymbol{W}_i & \boldsymbol{0} & 2\boldsymbol{T} & * & * \\
\boldsymbol{A}_i\boldsymbol{Q}_i+\boldsymbol{B}_i\boldsymbol{W}_i & \alpha_i\boldsymbol{B}_i & \boldsymbol{B}_i & \boldsymbol{Q}_l & * \\
\boldsymbol{W}_i & \boldsymbol{0} & \boldsymbol{0} & \boldsymbol{0} & \frac{\alpha_i}{\sigma^2}\boldsymbol{I}
\end{pmatrix}>0,\ for\ \ l\in\wp_0,(i,l)\in\Omega, \tag{33b}$$

then, the globally asymptotically stable of PWA system (1) is achieved under the event-triggering strategy (15).

Proof The proof of Corollary 1 is similar as the proof of Theorem 1 by using $\boldsymbol{\upsilon}=\boldsymbol{\omega}$ such that $\boldsymbol{H}_i=\boldsymbol{K}_i, \boldsymbol{g}_i=\boldsymbol{m}_i$ which is a global generalized sector condition. It is obvious that Lemma 1 is verified $\forall\boldsymbol{x}\in S(\boldsymbol{\upsilon}-\boldsymbol{\omega},-\boldsymbol{u}_0,\boldsymbol{u}_0)$ [30]. □

Remark 6 In the case of global stability, the domain of attraction is the whole state space of the system. So there is no need to describe the domain of attraction. For the global case, considering $\boldsymbol{\upsilon}=\boldsymbol{\omega}$, the sector condition (12) in Lemma 1 is globally satisfied.

The controller gains $\boldsymbol{K}_i, \boldsymbol{m}_i, i\in\wp$ and corresponding domains of attraction can be obtained by solving the LMIs in Theorem 1. However, we hope to the domain of attraction as large as possible. Therefore, an optimization problem can be proposed by minimizing $\mathrm{tr}(\boldsymbol{P}_i), i\in\wp$. Based on the discussion above, the optimization problem can be described as

Problem 2 *For a given σ in the event-triggering condition (6) design an event-triggered controller (5) that guarantees the domain of attraction is maximized.*

A solution to Problem 2 is given by solving the following optimization problem:

$$\min_{W_i\ Q_i}\ \mathrm{tr}(\boldsymbol{Q}_i^{-1}),\quad i\in\wp\ \ \text{subject to (18}a\text{), (18}b\text{)and(19)} \tag{34}$$

Remark 7 The trace of $\boldsymbol{Q}_i^{-1}$ is an convex function [32]. Hence, the optimization problem can be effectively solved by using the toolbox CVX in MATLAB [33].

4 Numerical examples

Examples are considered to show the effectiveness of the approach proposed in this paper. We consider two examples: One is an inverted pendulum model, and the other one is the tunnel diode model. The PWA systems are modeled by approximate linearization methods. Then, the discrete-time PWA systems can be obtained by discretization. Using Theorem 1 in Sect. 3, we can obtain the feedback gains $\boldsymbol{K}_i$ and $\boldsymbol{m}_i$ of the each subsystem and the domain of attraction is estimated. The maximal domain of attraction can be obtained by solving optimization problem 2. We compare the simulation results for σ having different values. The update rate is defined as the ratio of the number of events that occur and the total number of measurements.

Example 1 Consider the inverted pendulum system as shown in Fig. 3 which is the actual model of inverter pendulum. θ indicates angular displacement of pendulum. Let $\left(x_1\ x_2\right)^T = \left(\theta\ \dot{\theta}\right)^T$. The inverter pendulum model with saturation level $\boldsymbol{u}_0 = 5$ is considered as [34]:

$$\begin{cases} \dot{x}_1 = x_2 \\ \dot{x}_2 = -0.1x_2 + \sin(x_1) + \mathrm{sat}(u) \end{cases}$$

The characteristic of nonlinear function $\sin(x_1)$ is modeled by PWA function. The approximation effect is shown in Fig. 4. The approximation of the equation is described by

$$sin(x_1) = \begin{cases} -0.85x_1 - 2.6, & -4 < x_1 < -2 \\ -0.9, & -2 < x_1 < -1 \\ 0.9x_1, & -1 < x_1 < 1 \\ 0.9, & 1 < x_1 < 2 \\ 2.6 - 0.85x_1, & 2 < x_1 < 4. \end{cases}$$

Therefore, the discrete model parameters of each subsystem are, respectively,

$$\boldsymbol{A}_1 = \begin{pmatrix} 0.9958 & 0.0994 \\ -0.0845 & 0.9858 \end{pmatrix}, \quad \boldsymbol{B}_1 = \begin{pmatrix} 0.0050 \\ 0.0994 \end{pmatrix},$$

$$\boldsymbol{a}_1 = \begin{pmatrix} -0.0129 \\ -0.2583 \end{pmatrix}, \qquad \boldsymbol{x} \in \boldsymbol{\chi}_1$$

$$\boldsymbol{A}_2 = \begin{pmatrix} 1 & 0.0995 \\ 0 & 0.9900 \end{pmatrix}, \quad \boldsymbol{B}_2 = \begin{pmatrix} 0.0050 \\ 0.0994 \end{pmatrix},$$

$$\boldsymbol{a}_2 = \begin{pmatrix} -0.0045 \\ -0.0896 \end{pmatrix}, \qquad \boldsymbol{x} \in \boldsymbol{\chi}_2$$

$$\boldsymbol{A}_3 = \begin{pmatrix} 1.0045 & 0.0997 \\ 0.0897 & 0.9945 \end{pmatrix}, \quad \boldsymbol{B}_3 = \begin{pmatrix} 0.0050 \\ 0.0994 \end{pmatrix},$$

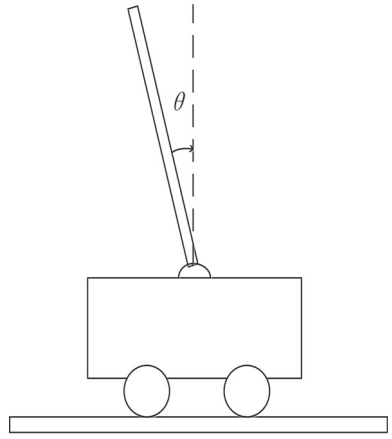

Fig. 3 Inverted pendulum

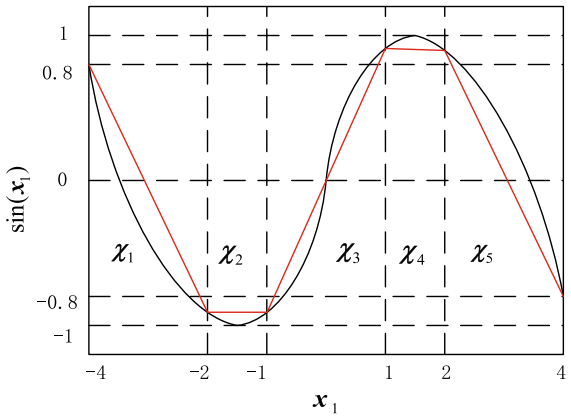

Fig. 4 PWA approximation of $\sin(x_1)$

$$\boldsymbol{a}_3 = \begin{pmatrix} 0 \\ 0 \end{pmatrix}, \qquad \boldsymbol{x} \in \boldsymbol{\chi}_3$$

$$\boldsymbol{A}_4 = \begin{pmatrix} 1 & 0.0995 \\ 0 & 0.9900 \end{pmatrix}, \quad \boldsymbol{B}_4 = \begin{pmatrix} 0.0050 \\ 0.0994 \end{pmatrix},$$

$$\boldsymbol{a}_4 = \begin{pmatrix} 0.0045 \\ 0.0896 \end{pmatrix}, \qquad \boldsymbol{x} \in \boldsymbol{\chi}_4$$

$$\boldsymbol{A}_5 = \begin{pmatrix} 0.9958 & 0.0994 \\ -0.0845 & 0.9858 \end{pmatrix}, \quad \boldsymbol{B}_5 = \begin{pmatrix} 0.0050 \\ 0.0994 \end{pmatrix},$$

$$\boldsymbol{a}_5 = \begin{pmatrix} 0.0129 \\ 0.2583 \end{pmatrix}, \qquad \boldsymbol{x} \in \boldsymbol{\chi}_5.$$

The five domains of the system can be described by ellipsoids (3), and the corresponding parameters are $\boldsymbol{E}_1 = \left(1, 0\right), f_1 = 3$, $\boldsymbol{E}_2 = \left(2, 0\right), f_2 = 3$, $\boldsymbol{E}_3 = \left(1, 0\right), f_3 = 0$, $\boldsymbol{E}_4 = \left(2, 0\right), f_4 = -3$, $\boldsymbol{E}_5 = \left(1, 0\right), f_5 = -3$. By applying Theorem 1, the feedback gains (consider $\sigma = 0.3$) are, respectively,

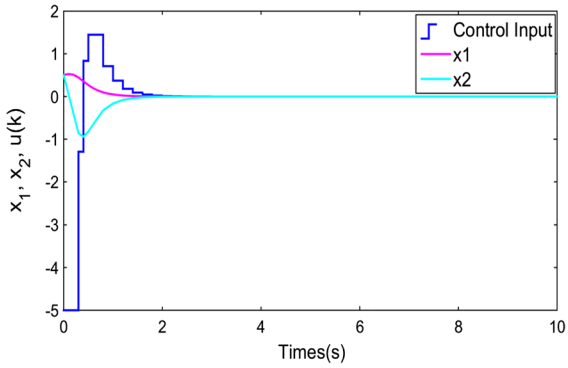

Fig. 5 Simulations of the state and saturated control input sat($\boldsymbol{u}$)

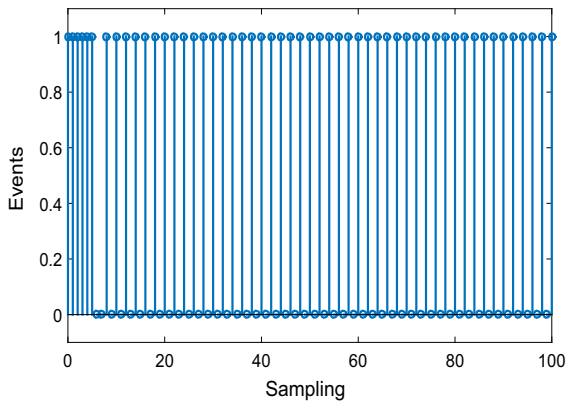

Fig. 6 The event is triggered with $\sigma = 0.3$

$$\boldsymbol{K}_1 = \begin{pmatrix}-16.0805 & -7.8301\end{pmatrix}, \quad \boldsymbol{m}_1 = 4.5255$$
$$\boldsymbol{K}_2 = \begin{pmatrix}-16.6310 & -9.1267\end{pmatrix}, \quad \boldsymbol{m}_2 = 5.9048$$
$$\boldsymbol{K}_3 = \begin{pmatrix}-16.8699 & -7.2586\end{pmatrix}, \quad \boldsymbol{m}_3 = 0$$
$$\boldsymbol{K}_4 = \begin{pmatrix}-16.6310 & -9.1267\end{pmatrix}, \quad \boldsymbol{m}_4 = -5.9048$$
$$\boldsymbol{K}_5 = \begin{pmatrix}-16.2014 & -7.8720\end{pmatrix}, \quad \boldsymbol{m}_5 = -4.4509,$$

and the Lyapunov matrices can be obtained as

$$\boldsymbol{P}_1 = \begin{pmatrix}5.2362 & 0.5641\\ 0.5641 & 0.2632\end{pmatrix}, \boldsymbol{P}_2 = \begin{pmatrix}5.5719 & 0.5432\\ 0.5432 & 0.2611\end{pmatrix},$$
$$\boldsymbol{P}_3 = \begin{pmatrix}4.9696 & 0.6619\\ 0.6619 & 0.2309\end{pmatrix}, \boldsymbol{P}_4 = \begin{pmatrix}5.5719 & 0.5432\\ 0.5432 & 0.2611\end{pmatrix},$$
$$\boldsymbol{P}_5 = \begin{pmatrix}5.2216 & 0.5589\\ 0.5589 & 0.2594\end{pmatrix}.$$

Figures 5, 6, and 7 show the simulation results by using Theorem 1. The simulation time is 10 seconds. Under the initial condition $\boldsymbol{x}(0) = \begin{pmatrix}0.5 & 0.5\end{pmatrix}^T$, the simulations of state and saturated controller are shown in Fig. 5. As can be seen from Fig. 5, the states of the system and controller which is saturated converge to the origin. Event triggers are shown in Fig. 6 (the "0" is not triggered, and the "1" is triggered). Meanwhile, Fig. 7 shows the domain of attraction with different parameters σ. Especially, the figure (a) shows the domain of attraction that we estimated using the ellipsoid, and the figure (b) shows the domain of attraction corresponding to the region decided by the range of state x_1 in Example 1 using Theorem 1. It can be seen that the estimated domain of attraction becomes smaller as the parameter σ becomes larger due to the fewer number of event triggers. Table 1 contains a comparison of the update rate with different event-trigger parameters σ.

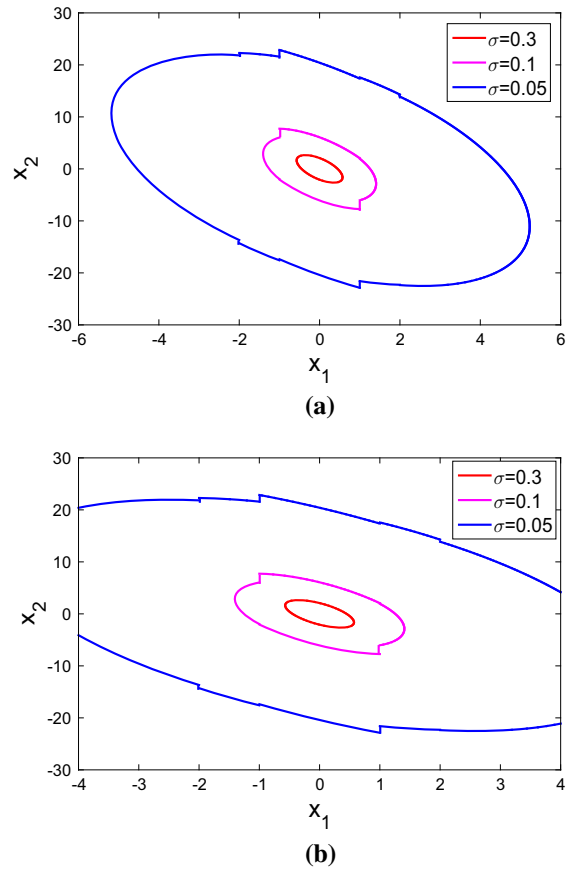

Fig. 7 Estimated domains of attraction with different σ in event-triggering condition (6)

Table 1 Comparison of different update rates with different σ in Example 1

σ	0.05	0.1	0.3	0.5	0.7
Update rate	98%	94%	58%	49%	29%

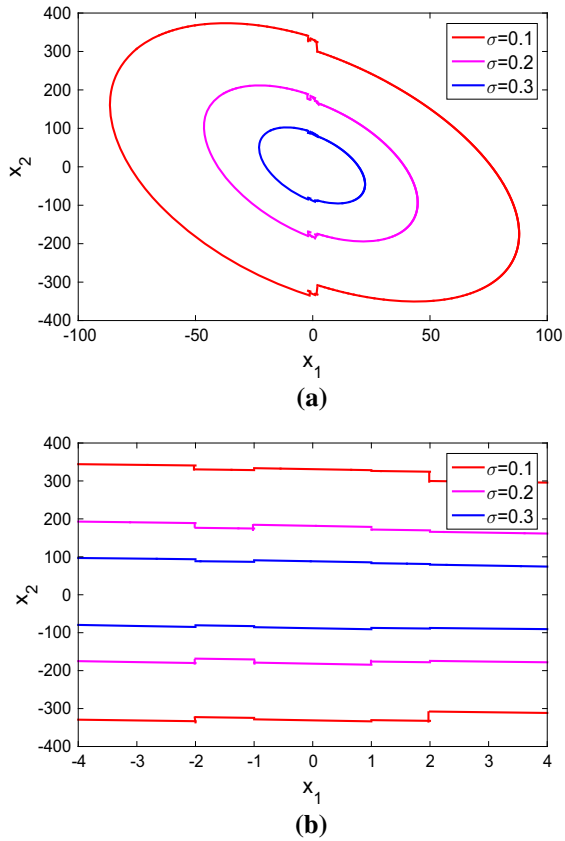

Fig. 8 Domains of attraction by solving optimization problem for different σ

It gives evidence that the event-triggered control leads to great effect in terms of the reduction of the waste of resources.

Next, we solve the corresponding optimization problem and the corresponding Lyapunov matrices can be obtained as (considering $\sigma = 0.3$)

$$\boldsymbol{P}_1 = \begin{pmatrix} 0.0025 & 2.7140 \times 10^{-4} \\ 2.7140 \times 10^{-4} & 1.2457 \times 10^{-4} \end{pmatrix},$$

$$\boldsymbol{P}_2 = \begin{pmatrix} 0.0028 & 2.8010 \times 10^{-4} \\ 2.8010 \times 10^{-4} & 1.3892 \times 10^{-4} \end{pmatrix},$$

$$\boldsymbol{P}_3 = \begin{pmatrix} 0.0025 & 3.5142 \times 10^{-4} \\ 3.5142 \times 10^{-4} & 1.2837 \times 10^{-4} \end{pmatrix},$$

$$\boldsymbol{P}_4 = \begin{pmatrix} 0.0028 & 2.8010 \times 10^{-4} \\ 2.8010 \times 10^{-4} & 1.3892 \times 10^{-4} \end{pmatrix},$$

$$\boldsymbol{P}_5 = \begin{pmatrix} 0.0026 & 2.8994 \times 10^{-4} \\ 2.8994 \times 10^{-4} & 1.4239 \times 10^{-4} \end{pmatrix}.$$

With these values, less conservativeness can be obtained as shown in Fig. 8. The figure (b) in Fig. 8 represents the domain of attraction corresponding to the region decided by the range of state x_1 in Example 1 by solving Problem 2. Compared to the results obtained from Theorem 1, it can be seen that the domain of attraction obtained by solving optimization problem 2 is always larger than the ones from Theorem 1. This proves the effectiveness of the optimization problem that we proposed.

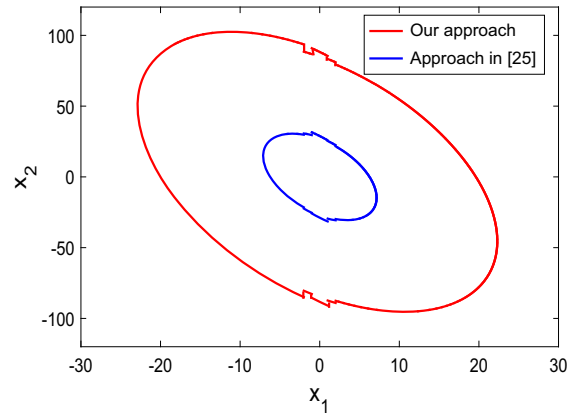

Fig. 9 The comparison of domain of attraction with Literature [27] under the same parameter $\sigma = 0.3$

Figure 9 shows the domain of attraction by comparing the optimization method proposed in Problem 2 with the literature [27] optimization method. The red line indicates the domain of attraction obtained by solving the optimization Problem 2, and the blue line indicates the domain of attraction obtained by solving the optimization problem in the literature [27]. It can be clearly seen that the domain of attraction obtained by using our optimization method is obviously larger than by using the method in literature [27]. The advantages of our optimization method are proved.

Example 2 Consider the follow tunnel diode (Fig. 10) [35,36].

$$\dot{\boldsymbol{x}} = \begin{pmatrix} -30 & -20 \\ 0.05 & 0 \end{pmatrix} \boldsymbol{x} + \begin{pmatrix} 24 \\ -50g(x_2) \end{pmatrix} + \begin{pmatrix} 20 \\ 0 \end{pmatrix} \boldsymbol{u}. \quad (35)$$

The nonlinear function $g(x_2)$ is modeled by PWA function. The approximation effect is shown in Fig. 11, and the polytopic regions can be generated as

$$\boldsymbol{\chi}_1 = \{\boldsymbol{x} \in \mathbb{R}^2 | -L < x_2 < 0.2\},$$

$$\boldsymbol{\chi}_2 = \{\boldsymbol{x} \in \mathbb{R}^2 | 0.2 < x_2 < 0.6\},$$

$$\boldsymbol{\chi}_3 = \{\boldsymbol{x} \in \mathbb{R}^2 | 0.6 < x_2 < L\},$$

where L is set to 1×10^4.

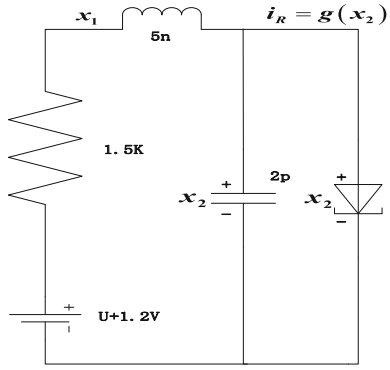

Fig. 10 Tunnel diode circuit

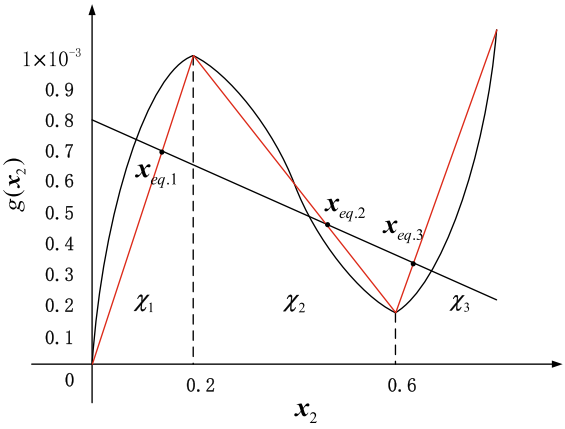

Fig. 11 PWA approximation of $g(x_2)$

We aim at designing a controller that stabilizes the system to equilibrium point $\boldsymbol{x}_{eq.3} = \left(0.3714\ 0.6429\right)^T$ of $\boldsymbol{\chi}_3$ in the presence of input saturation. The three domains of the system can be described by ellipsoids, and the corresponding parameters are $\boldsymbol{E}_1 = \left(0, 0.0002\right)$, $\boldsymbol{f}_1 = 1$, $\boldsymbol{E}_2 = \left(0, 5\right)$, $\boldsymbol{f}_2 = 1.2143$, $\boldsymbol{E}_3 = \left(0, 0.0002\right)$, $\boldsymbol{f}_3 = -1$. The simulation time is 10 seconds, and the initial state is $\boldsymbol{x}(0) = \left(0.5\ 1\right)^T$.

The state responses and control input of the system are shown in Fig. 12. The state stabilizes to equilibrium point $\boldsymbol{x}_{eq.3} = \left(0.3714\ 0.6429\right)^T$ and control effect converges to zero. Especially, the control effect can be clearly observed in figure (b) of Fig. 12 with the simulation time of 2 seconds. Table 2 gives the results from the application of Theorem 1 with the variation of the update rate under different values of σ. Figure 13 shows the corresponding domains of attraction with different σ by solving the optimization problem. The figure (b) in Fig. 13 is the domain of attraction made local magnification of the left figure in Fig. 13 in the second subsystem $\boldsymbol{\chi}_2 = \{\boldsymbol{x} \in \mathbb{R}^2 | 0.2 < x_2 < 0.6\}$. A larger domain of attraction can be obtained by choosing a smaller σ, while the number of controller updates has increased.

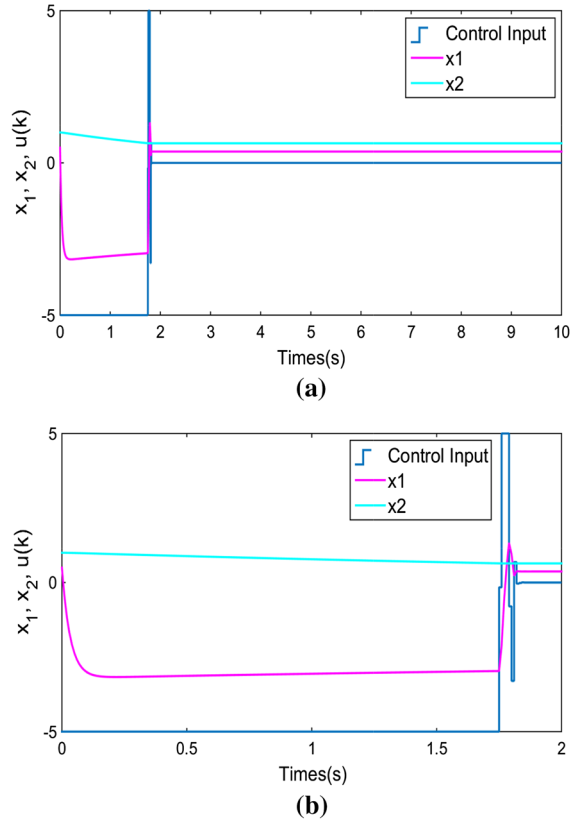

Fig. 12 Simulations of the state and saturated control input sat($\boldsymbol{u}$)

Table 2 Comparison of different update rates with different σ in Example 2

σ	0.05	0.08	0.1	0.2
Update rate	88.2%	15.5%	13%	6.3%

5 Conclusion

In this paper, by introducing the nonlinear dead-zone function, we transform the problem of saturation into solving the problem of nonlinear dead-zone function. We first propose an event-triggering strategy and approach of controller synthesis for PWA systems subject to input saturation. The controller gains are

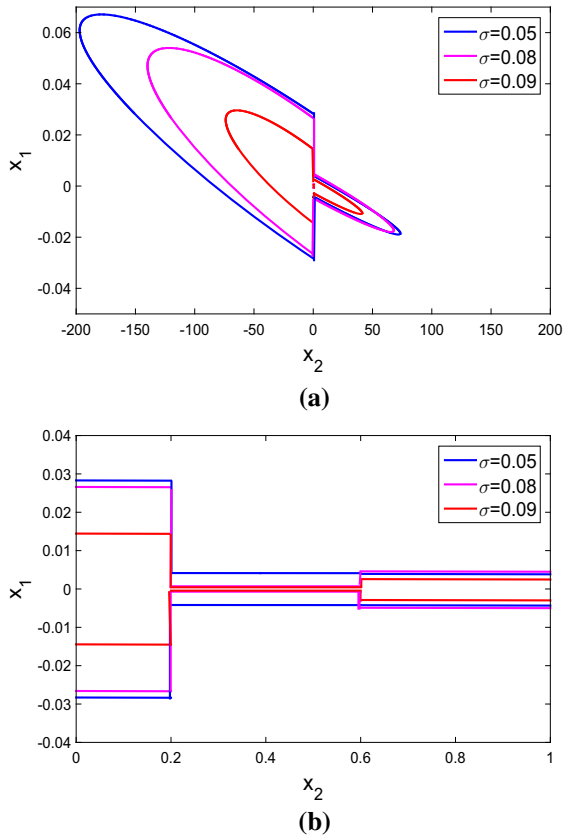

Fig. 13 Domains of attraction by solving optimization problem for different σ

obtained by solving the LMIs, and the domain of attraction is estimated. This approach guarantees regional asymptotic stability for given a initial condition for PWA systems. We also extend the approach to achieve global asymptotic stability. Further, the optimization problem for obtaining the maximal domain of attraction is achieved.

For future research, the event-triggered control of PWA systems will be discussed by combining input constraints and state constraints. In addition, the convex hull method is used to deal with input saturation. Comparing the advantages and disadvantages of two methods is also our future consideration.

Acknowledgements This work is supported by National Natural Science Foundation of China [61807016 and 61473136]. This work is also partially supported by the Jiangsu Province Postdoctoral Fund of China [1701095B], the Fundamental Research Funds for the Central University [JUSRP51733B] and Natural Science Foundation of Jiangsu Higher Education Institutions of China [18KJB180026], China Postdoctoral Science Foundation (2018M642160) and the 111 Project (B12018).

Compliance with ethical standards

Conflict of interest The authors declare that they have no conflict of interest concerning the publication of this manuscript.

References

1. Årzén, K.E., Cervin, C., Henriksson, D.: Resource-constrained embedded control systems: possibilities and research issue. In: Proceedings of the Co-Design of Embedded Real-Time Systems Workshop (2003)
2. Tabuada, P.: Event-triggered real-time scheduling of stabilizing control tasks. IEEE Trans. Autom. Control **52**(4), 1680 (2007)
3. Lehmann, D., Lunze, J.: Event-based output-feedback control, Control & Automation pp. 982–987 (2011)
4. Stöcker, C., Lunze, J.: Event-based control of nonlinear systems: an input–output linearization approach. IEEE Conf. Dec. Control Eur. Control Conf. **413**(1), 2541 (2011)
5. Wu, W., Reimann, S., Liu, S.: Event-triggered control for linear systems subject to actuator saturation. IFAC Proc. Vol. **47**(3), 9492 (2014)
6. Årzén, K.E.: A simple event-based PID controller. In: Proceedings of the 14th IFAC World Congress (1999)
7. Heemels, W.P.M.H., Donkers, M.C.F., Teel, A.R.: Periodic event-triggered control for linear systems. IEEE Trans. Autom. Control **58**(4), 847 (2013)
8. Souza, M., Deaecto, G.S., Geromel, J.C., Daafouz, J.: Self-triggered linear quadratic networked control. Optim. Control Appl. Methods **35**, 524–538 (2013). https://doi.org/10.1002/oca.2085
9. Heemels, W.P.M.H., Johansson, K.H., Tabuada, P.: An introduction to event-triggered and self-triggered control. In: Proceedings of the 51th IEEE Conference on Decision and Control (2012)
10. Lou, X.Y., Li, Y., Sanfelice, R.G.: Robust stability of hybrid limit cycles with multiple jumps in hybrid dynamical systems. IEEE Trans. Autom. Control **63**(4), 1220 (2018)
11. Lou, X.Y., Jiang, Z.X.: Event-triggered control of spatially distributed processes via unmanned aerial vehicle. Int. J. Adv. Robot. Syst. **13**, 1 (2016)
12. Wu, W., Reimann, S., Görges, D., Liu, S.: Event-triggered control for discrete-time linear systems subject to bounded disturbance. Int. J. Robust Nonlinear Control **26**(9), 1902 (2016). https://doi.org/10.1002/rnc.3388
13. Wu, W., Reimann, S., Görges, D., Liu, S.: Suboptimal event-triggered control for time-delayed linear systems. IEEE Trans. Autom. Control **60**(5), 1386 (2015)
14. Moreira, L.G., Groff, L.B., De Silva Jr., J.M.G.: Event-triggered state-feedback control for continuous-time plants subject to input saturation. J. Control Autom. Electr. Syst. **27**(5), 1 (2016)
15. Zuo, Z.Q., Li, Q.S., Li, H.C., Wang, Y.J.: Co-design of event-triggered control for discrete-time systems with actuator saturation. In: Proceedings of the 2016 12th World Congress on Intelligent Control and Automation, pp. 170–175 (2016)

16. Johansson, M.: Piecewise Linear Control Systems. Springer, Berlin (2003)
17. Heemels, W., Schutter, B.D., Bemporad, A.: Equivalence of hybrid dynamical models. Automatica **37**, 1085 (2001)
18. Llibre, J., Novaes, D.D., Teixeira, M.A.: Maximum number of limit cycles for certain piecewise linear dynamical systems. Nonlinear Dyn. **82**(3), 1 (2015)
19. Wu, T., Wang, L., Yang, X.S.: Chaos generator design with piecewise affine systems. Nonlinear Dyn. **84**(2), 817 (2016)
20. Kulkarni, V., Jun, M., Hespanha, J.: Piecewise quadratic Lyapunov functions for piecewise affine time-delay systems. In: Proceedings of the American Control Conference, vol. 5, pp. 3885–3889 (2004)
21. Chen, Y., Sun, Y., Tang, C.S., Su, Y.G., Hu, A.P.: Characterizing regions of attraction for piecewise affine systems by continuity of discrete transition functions. Nonlinear Dyn. **90**(3), 2093 (2017)
22. Miad, M., Luis, R.: Asymptotic stability of sampled-data piecewise affine slab systems. Pergamon Press Inc, Oxford (2012)
23. Iervolino, R., Vasca, F.: Cone-copositivity for absolute stability of lur'e systems, Decision and Control pp. 6305–6310 (2014)
24. Iervolino, R., Vasca, F., Tangredi, D.: Lyapunov stability for piecewise affine systems via cone-copositivity. Automatica **81**, 22 (2017)
25. Qiu, J.B., Wei, Y.L., Karimi, H.R., Gao, H.J.: Reliable control of discrete-time piecewise-affine time-delay systems via output feedback. IEEE Trans. Reliab. **67**(99), 1 (2017)
26. Bardakci, I.E., Lee, J., Lagoa, C.: Robust stabilization of discrete-time piecewise affine systems subject to bounded disturbances. In: Proceedings of the IEEE 55th Conference on Decision and Control, pp. 7252–7257 (2016)
27. Chen, Y., Zhou, Q., Fei, S.: Robust stabilization and L_2-gain control of uncertain discrete-time constrained piecewise-affine systems. Nonlinear Dyn. **75**(1–2), 127 (2014)
28. Rodriguesa, L., Boyd, S.: Piecewise-affine state feedback for piecewise-affine slab systems using convex optimization. Syst. Control Lett. **54**, 835 (2005)
29. Rodrigues, L., Boukas, E.K.: Piecewise-linear H_∞ controller synthesis with applications to inventory control of switched production systems. Automatica **42**(8), 1245 (2006)
30. Tarbouriech, S., Garcia, G., da Silva Jr., J.M.G., Queinnec, I.: Stability and Stabilization of Linear Systems with Saturating Actuators. Springer, London (2011)
31. Branicky, M.S.: Multiple lyapunov functions and other analysis tools for switched and hybrid systems. IEEE Trans. Autom. Control **43**, 475 (1998)
32. Boyd, S., Vandenberghe, L.: Convex Optimization. Cambridge University Press, Cambridge (2004)
33. Grant, M., Boyd, S.: CVX: Matlab Software for Disciplined Convex Programming, version 2.0 beta (2013)
34. Rantzer, A., Johansson, M.: Piecewise linear quadratic optimal control. IEEE Trans. Autom. Control **45**(4), 629 (2000)
35. Hassibi, A., Boyd, S.: In: Proceedings of the American Control Conference, vol. 6, pp. 3659–3664 (1998)
36. Rodrigues, L.: In state feedback control of piecewise-affine systems with norm bounded noise, vol. 3. In: Proceedings of the American Control Conference, vol. 3, pp. 1793–1798 (2005)